



# Impact of Pyrolysis Temperature and Application Amount of Sewage Sludge Biochar on the Speciation and Bioavailability of Cd and Pb in Paddy Soil

Huan Wang · Lei Zhou · Yitong Dan · Xiaoxia Wang · Yin Zhu Diao · Feihong Liu · Wengjing Sang

Received: 19 January 2022 / Accepted: 14 May 2022 / Published online: 1 June 2022  
© The Author(s), under exclusive licence to Springer Nature Switzerland AG 2022

**Abstract** In order to investigate the effect of various pyrolysis temperatures and application amount on the remediation of Cd–Pb contaminated soil, dried sewage sludge was pyrolyzed at 300 °C (SSB300) and 500 °C (SSB500), and soil incubation experiments were conducted for 60 days with two biochars (SSB300 and SSB500) and three different application amounts (1%, 3%, and 5%). The chemical speciation and bioavailability of Cd and Pb in paddy soil were determined by BCR and DTPA. Results showed that sewage sludge-based biochar (SSB) slightly increased the soil pH, due to the neutral SSB. The specific surface area of SSB500 was increased by 40.06 m<sup>2</sup>/g compared to SSB300. FTIR showed a decrease in the hydroxyl vibrational peak of SSB500 compared to SSB300; in addition, the intensity of the aliphatic-CH<sub>2</sub> peak decreased with increasing pyrolysis temperature, indicating a decrease in non-polar aliphatic functional groups on the surface of SSB. The incubation experiments showed that the addition of 5% SSB500 had the best performance for

DTPA-extractable Cd (48 mg.kg<sup>-1</sup> to 12.81 mg.kg<sup>-1</sup>) and Pb (90.23 mg.kg<sup>-1</sup> to 15.91 mg.kg<sup>-1</sup>). And 5% SSB500 amendment more remarkably transformed Cd and Pb from the acid-soluble state to the residual state than other treatments, demonstrating that the high pyrolysis temperature and application amount had great influence for transformation of Cd and Pb. In addition, the microbial community in the soil was significantly changed by 5% SSB500 application. At the phylum level, *Chloroflexi* is the dominant species, due to its strong tolerance in Cd-contaminated soil. At the genus level, the relative abundance of *Thiobacillus* and *Deftuviicoccus* increased, which would enhance inorganic ion transport and metabolism functions to promote passivation and stabilization of heavy metals throughout the remediation process.

**Keywords** Sewage sludge biochar · Immobilization · Pyrolysis temperature · Application amount · Microbial community

**Supplementary Information** The online version contains supplementary material available at <https://doi.org/10.1007/s11270-022-05659-w>.

H. Wang · L. Zhou · Y. Dan · X. Wang · Y. Diao · F. Liu · W. Sang (✉)

Textile Pollution Controlling Engineering Center of Ministry of Environmental Protection, College of Environmental Science and Engineering, Donghua University, Shanghai 201620, China  
e-mail: wjsang@dhu.edu.cn

## 1 Introduction

In recent years, agricultural soil contamination by heavy metals (such as Cd and Pb) has become a significant concern due to its high mobility and easy accumulation in crops (Yang, et al., 2018). Cd and Pb are usually released into the soil by human activities such as excessive agricultural inputs, wastewater

irrigation, coal combustion, mining, and smelting (Quan, et al., 2021). An intensive national soil survey in China showed that 19.4% of the agricultural soil samples (equivalent to about 26 million ha) were contaminated with Cd and Pb during 2005 and 2013 (Zhao, et al., 2015). Cd and Pb have negative effects on organisms, including the potential induction of a series of physiological and neurological disorders (Buha, et al., 2018; Khanam, et al., 2020). Therefore, sustainable management of paddy soil to reduce the simultaneous mobilization and utilization of Cd and Pb has become an urgent issue. Many techniques have been developed for the remediation of heavy metals in soil, including electrokinetic remediation (Wang, Sun, et al., 2021), phytomicrobial remediation (Mishra, et al., 2021; Thakare, et al., 2021), biochar fixation remediation (Wang, Shi, et al., 2021), and clay mineral adsorption (Otunola and Ololade, 2020). Compared to these traditional soil remediation methods, biochar enhancement is a very perspective technology because of its high efficiency and low cost (Wang, Shen, et al., 2021). The practice of biochar to immobilize heavy metals in soil by reducing their mobility and bioavailability has been widely reported (Beckers, et al., 2019; Jörg, et al., 2020).

Research has mainly focused on the production of biochar from agricultural and forestry waste and animal manure, which have shown potential as metal adsorbents with higher adsorption capacity in soil (Hopkins and Hawboldt, 2020; Eikelboom, et al., 2018). Nowadays, biochar produced from sewage sludge feedstock is considered as an attractive multiple functional material for heavy metal stabilization and soil quality improvement (Liu, Gong, et al., 2020). Sewage sludge is a popular feedstock for biochar preparation and has attracted much attention due to its high mineral content (Lam, et al., 2020). SSB is commonly used for soil amendment (Liu, Huang, et al., 2021), which provided a sustainable pathway for the ever-increasing resourcefulness of sludge (Tomczyk, et al., 2020). Islam et al. (2021) found that that pulp mill sludge biochar had a larger specific surface area, richer functional groups (Islam, et al., 2021), and stronger heavy metal adsorption capacity than rice straw biochar. Soil physicochemical properties such as soil pH, cation exchange capacity, and organic matter content have influence on the solidification and stabilization of heavy metal by biochar in soil (Shentu,

et al., 2022). For example, application of biochar to acidic contaminated soil raised the pH of the soil (Fang, et al., 2016; Mansoor, et al., 2021). Shentu et al. (2022) investigated the effects of groundwater level fluctuations on the dispersion and morphology of Cu, Ni, Pb, and Zn by column experiments, which found that the stability of heavy metals in the fluctuating and seated zones was better than that in the unsaturated zone (Shentu et al., 2022). Due to the complexity of the soil environment (microbial communities), integrated considerations were often required in pollution control. Microorganisms such as *Pseudomonas syringe*, *Escherichia coli*, *Bacillus*, and *Staphylococcus* could enrich and precipitate stable processes of heavy metals (Yang et al., 2021a). Because of microbial metabolic processes, heavy metals would precipitate and be slightly chelated on soluble or insoluble macromolecules. Although microorganisms in contaminated soil were resistant to heavy metals, their low activity or insufficient number of microorganisms often makes their remediation capacity insufficient. Therefore, the regulation and coupling effect of biochar on soil microorganisms during soil heavy metals immobilization are receiving increasing attention (Tian, et al., 2020).

The most important factor determining the effectiveness of sludge biochar remediation is the diversity of its physicochemical properties (Kong, et al., 2021). One of the critical factors is pyrolysis temperature. Higher pyrolysis temperatures can reduce the H and O content, increase the ash and carbon, and change the surface structure or functional groups, which can greatly change the properties of biochar (Qu, et al., 2020; Xing, et al., 2019). Liu, Graham, et al. (2021) investigated the effect of different pyrolysis biochar on Cd and Pb in soil by using HNO<sub>3</sub>-treated oxidized balsam at 300 and 600 °C and the results showed a 6.9-times and 5.6-times higher uptake capacities, respectively (Liu, Graham, et al., 2021). In addition, municipal sludge biochar is rich in heavy metals and would release into the soil over time, which could lead to secondary contamination of the soil (Wang, et al., 2020). Thus, application amount of biochar in remediation process became an important factor (de Figueiredo, et al., 2019). Irfan et al. (2021) have studied 0%, 2%, 4%, and 6% (w/w) biochar application in farm topsoil (0–20 cm) and found that 6% biochar application was most efficient in declining the bioavailability of Pb, Cd, and Cr (Irfan, et al., 2021). The

above studies suggested that pyrolysis temperature and application amount were essential factors to be conducted to stabilize heavy metals. However, there were few studies to focus on the combined effects of pyrolysis temperature, application amount, and microbial community on the passivation and stabilization of heavy metals in soil.

In this study, SSB300 and SSB500 were pyrolyzed with municipal sludge at 300 °C and 500 °C, respectively. Sixty-day soil incubation experiments were conducted to simulate the complex Cd–Pb immobilization process in paddy soil by different application amount (1%, 3%, 5%) of SSB300 and SSB500. During the soil incubation experiments, the bioavailability and speciations of Cd and Pb were evaluated by DTPA and BCR. Furthermore, the effects of SSB on the abundance of microorganisms and the diversity of microorganisms in Cd–Pb complex contaminated soil were investigated by high-throughput sequencing (HTS) of the 16S rRNA gene and principal component analysis (PCA). This work will provide a theoretical foundation for the application of SSB in Cd/Pb-contaminated soil.

## 2 Materials and Methods

### 2.1 Sample Collection and Biochar Preparation

The soil was collected from a rice field in Songjiang District, Shanghai (121°9′25″E 31°5′13″N), and then dried and passed through a 10-mesh sieve and refrigerated. The physicochemical properties of the soil are shown in Table S1. Municipal sewage sludge was obtained from Shanghai Songjiang Sewage Treatment Plant. The feedstock was dried in an oven at 105 °C for 48 h and then fully ground and sieved through 60 mesh. A certain amount of feedstock was weighed and put into a vacuum tube furnace for pyrolysis at a heating rate of 10 °C/min. The pyrolysis temperature was fixed at 300 °C and 500 °C for 2 h.

The pH of SSB was measured by a pH meter (PHS-3C, Remagnet) at a ratio of 1:20 SSB/water (w/v). Ash content of SSB was calcined at 800 °C for 2 h in a muffle furnace. C, H, and N elements contained in the SSB were measured using an elemental analyzer (Vario EL III). Specific surface area of the SSB was measured by a fully automated rapid specific surface area and porosity analyzer (Autosorb-iQ,

Quadrasorb, USA). The infrared spectra of SSB were measured by FTIR (Nicolet 6700, Thermo, USA). The microscopic features of SSB were observed by SEM (S-4800, Hitachi, Japan).

### 2.2 Incubation Experiments and Sample Analysis

The incubation experiments were carried out in a constant temperature incubator (25 °C). Certain amounts of SSB300 and SSB500 were added to 600 g contaminated soil to achieve final application rates of 1%, 3%, and 5% (w/w). DI water was added to the mixture to achieve a final soil moisture level of 70% and then mixed thoroughly to achieve homogeneity. Water loss was replenished with DI water every 2 days. Soil samples were collected on 7, 15, 30, and 60 days for further analysis.

DTPA-extractable Cd and Pb in soil were analyzed (Sun, et al., 2021a) according to the method of Sun et al. (2021a). Cd and Pb fractions in the soil were analyzed by a modified BCR sequential extraction method (Gao, et al., 2020). The concentrations of Cd and Pb were analyzed by inductively coupled plasma-mass spectrometry (Z-2000, Hitachi, Japan).

### 2.3 High-Throughput Sequencing and Analysis

To investigate the microbial community diversity characteristics of soil samples after SSB500 addition, blank and soil with 5% SSB500 addition after 60-day incubation were collected for microbial community analysis by high-throughput sequencing (HTS) of 16S rRNA genes and principal component analysis at Meiji Biotechnology Co. polymerase chain reaction (PCR); amplification primers 338F (ACTCCTACG GGAGGCAGCAG) and 806R (GGACTACHVGGG TWTCTAAT) were used.

The amplified samples were sequenced, and the data were processed to remove bad sequence data and detect suspicious chimeras to obtain high quality bacterial sequence data. To enhance comparability between samples, OTU clustering was performed based on the similarity between sequences (similarity > 97%); community composition analysis and principal component analysis were performed on the data. The raw sequencing data has been uploaded into the NCBI database Sequence Read Archive (SRA) and the accession number is SUB11379370.

### 3 Results and Discussions

#### 3.1 SSB Characterization

Physicochemical properties of SSB300 and SSB500 are listed in Table 1. The SSB yield decreased from 69.14% to 52.97% as the temperature raised from 300 °C to 500 °C. The reduction in SSB yield was mainly due to the decomposition of more organic matter at higher temperatures (Yuan, et al., 2015). With the pyrolysis temperature increased, the mineral ash content of SSB enhanced. The ash contained oxides and carbonates of Na, K, Ca, and Mg, which were alkaline in aqueous solution, and the surface of SSB was rich in alkaline groups (-COO- and -O-), raising the pH of SSB (Meier, et al., 2017). Elemental analysis found that C, H, O, and N contains in the SSB500 were less than those in SSB300. The H/C, O/C, and (O+N)/C atomic ratios were usually used to estimate the hydrophilic, aromaticity, and polarity of the SSB (Yuan et al., 2015), respectively. It can be seen from Table 1 that the aromaticity and hydrophobicity of SSB raised and the polarity reduced with increasing pyrolysis temperature, which was consistent with previous research (She, et al., 2020).

The SSB300 and SSB500 surface functionality was analyzed by FTIR spectroscopy for revealing the functional group changes on the surface. As shown in Fig. 1, the spectra were compared to reflect the effect of pyrolysis temperature on the presence of various functional groups. The FTIR peak observed in SSB300 and SSB500 at approximately 3432 cm<sup>-1</sup> was assigned to O–H stretching of alcoholic or phenolic functional groups. The hydroxyl vibration peak of SSB500 reduced compared to SSB300; the higher pyrolysis temperatures detached the bound water and caused the hydrogen-bonded -OH to break. The stretching vibration peak of aliphatic -CH<sub>2</sub> was near 2925 cm<sup>-1</sup>. The intensity of the aliphatic -CH<sub>2</sub> peak also declined with increasing pyrolysis temperature, indicating a reduction in non-polar aliphatic functional groups on the surface of SSB. It was owing to

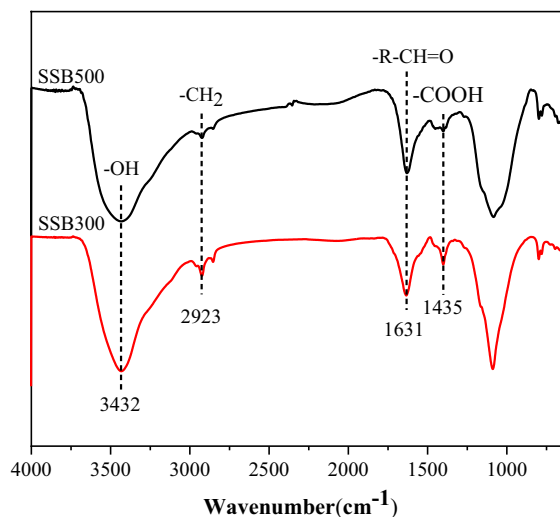


**Fig. 1** FTIR spectra of SSB

that most of the organic aliphatic hydrocarbons in the sludge decompose into gasses such as CH<sub>4</sub> and CO<sub>2</sub> at high temperatures, which increased the aromaticity of the SSB. The absorption peak at 1631 cm<sup>-1</sup> was the absorption peak stretching vibration of the amide carbonyl group, and the O–H bending vibration peak at 1450–1400 cm<sup>-1</sup> could be used as a determination of the presence of carboxylic acid compounds. The increase in pyrolysis temperature led to a decrease in aliphatic functional groups and an increase in aromatic structures in the sludge-derived biochar, which was consistent with the results reported by Zhang et al. (2022). The reason may be due to the aryl ring which was able to supply  $\pi$ -electron and form strong bond against heavy metal ion (Zhang, et al., 2022).

#### 3.2 Bioavailability of Cd and Pb

During the 60-day incubation, the change of DTPA-extractable Cd in the tested soil is displayed in Fig. 2 (a). The content of Cd bioavailability in the soil was significantly reduced with the addition of SSB. The stabilization efficiencies of Cd in soil at the 1%, 3%,

**Table 1** Basic physicochemical properties of SSB

SSB	Yield (%)	Ash (%)	pH	BET (m <sup>2</sup> /g)	C (%)	H (%)	O (%)	N (%)	H/C	O/C	(O+N)/C
SSB300	69.14	47.73	6.65	20.47	25.48	2.67	20.27	3.85	1.26	0.60	0.38
SSB500	52.97	67.25	7.30	60.53	20.36	1.05	8.30	3.04	0.62	0.31	0.22

and 5% application amount (SSB300) were 45.83%, 56.23%, and 67.61%, respectively. The stabilization efficiency of 1%, 3%, and 5% application rate (SSB500) for Cd in soil was 49.69%, 62.23%, and 70.61%, respectively. Obviously, the stabilization efficiency of 5% SSB500 for Cd was much better than 5% SSB300. The soil with 5% SSB500 application showed greatest impact, which was a 72.98% reduction in Cd bioavailability compared to the blank group (from 47.45 to 12.82 mg/kg). This was consistent with previous research (Zhu, et al., 2017). Figure 2 (b) reflects the effects of SSB application on the bioavailability of Pb in soil. Similarly, the content of Pb bioavailability was higher in SSB300-treated samples than in SSB500-treated samples. Possible reasons were the higher pyrolysis temperature of the SSB had more specific surface area and pore volume, which could provide more habitat for Cd and Pb (Yang et al., 2021b). Therefore, the higher the application amount, the greater reduction in the bioavailability of Pb. The bioavailability of Pb was reduced by 82.4% (from 90.23 to 15.91 mg/kg) in the soil after applied with 5% SSB500 in current research.

The main reason for the better passivation effect of SSB addition on heavy metals was that SSB possessed a large specific surface area, which enhanced the permeability of the soil and provided a suitable environment for microorganisms in the soil (Meier et al., 2017). In addition, due to the larger specific surface area of SSB300 and SSB500, it reduced the solubility of heavy metals by adsorption, and thus available reduced the migration of heavy metals in soil (She et al., 2020). Moreover, Li et al. (2020) reported that biochar contained a large number of organic functional groups (-C-OH, -C=O, COO-) and could complex with heavy metal Cd (II) or inorganic salt ions (Si, S<sup>2-</sup>, Cl<sup>-</sup>, etc.) (Li, et al., 2020). It was another reason why SSB reduced the bioavailability of Cd and Pb in soil. In agreement with the results of Zhou et al. (2017), the application of SSB in contaminated soil reduced the ecotoxicity and mobility of Cd and Pb in soil (Zhou, et al., 2017).

### 3.3 Speciation of Cd and Pb in Soil

The BCR method classifies the Cd state in soil into four speciation, including acid soluble, reducible, oxidizable, and residual state (Qureshi et al., 2020). Figure 3 shows the effect of different SSB treatments

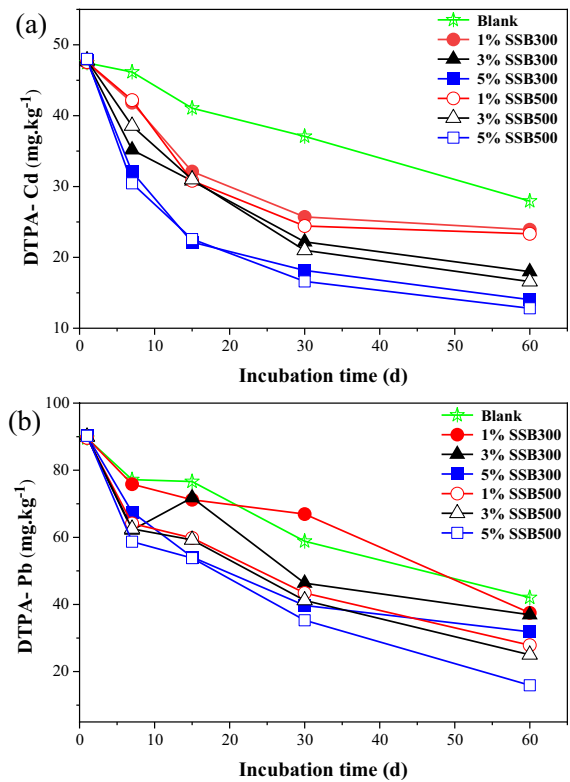
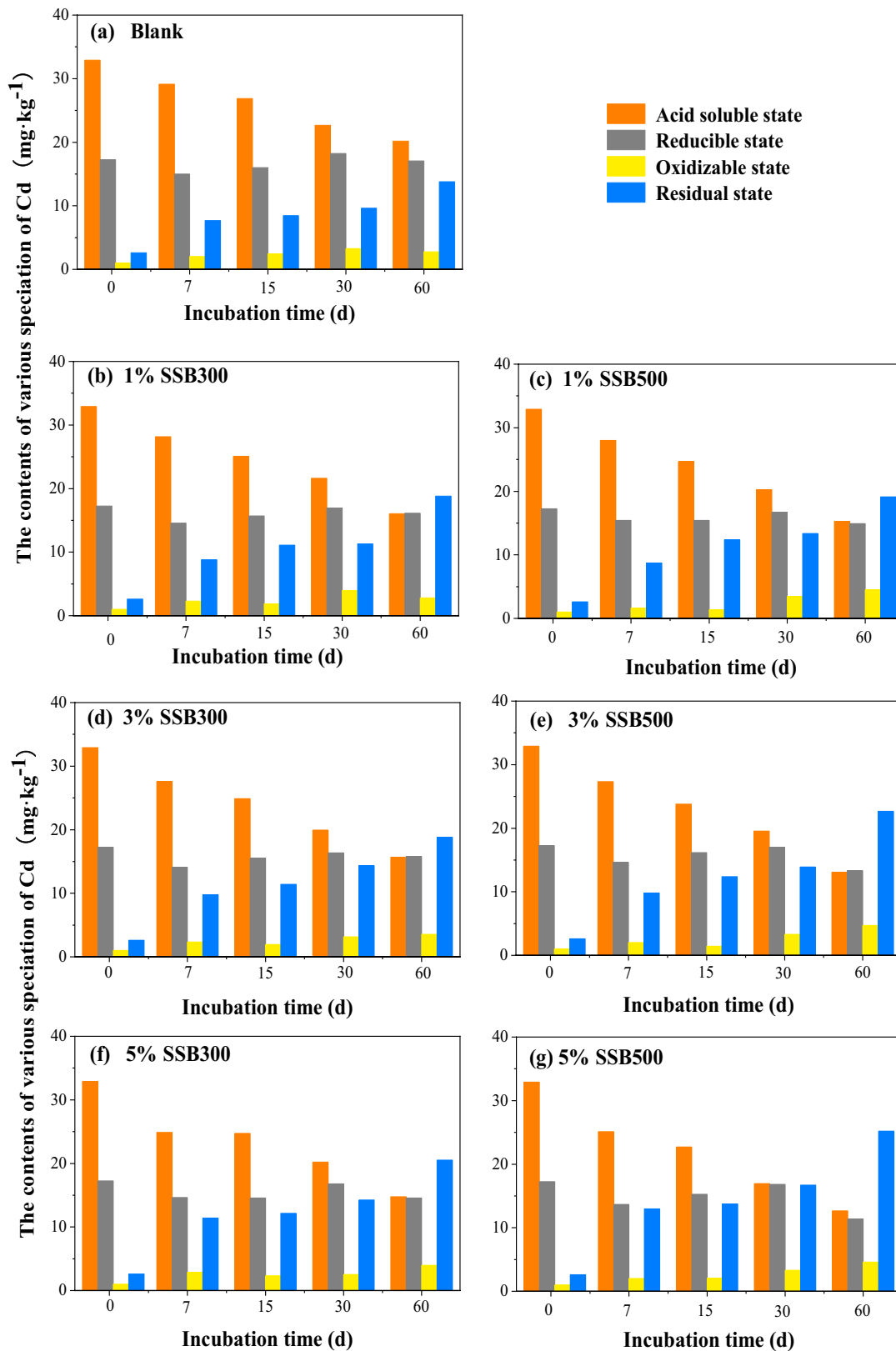


**Fig. 2** Effects of SSBs on the bioavailability of heavy metals. **a** Cd, **b** Pb

on the distribution of Cd morphology. For the blank treatment in Fig. 3(a), the main state of Cd in the initially contaminated soil (0-day) was acid soluble state, which accounted for about 53.83%. Acid soluble state reflected the toxicity of heavy metals and was easily absorbed by plants (Liu, Xiao, et al., 2020). After 60-day incubation, acid soluble state in the soil decreased from 29.13 mg/kg to 20.18 mg/kg. Residual state was the most stable state in the soil and had a crystalline structure of soil minerals that were not available to plants (Xu, et al., 2016). Residual state in the original contaminated soil increased from 7.67 mg/kg (0 day) to 13.79 mg/kg (60 days), due to the soil having self-purification function and stabilizing effect on heavy metals.

For the SSB treatments in Fig. 3(b)–(g), acid soluble state of Cd was significantly reduced and the residual state increased in the soil with SSB applications after 60-day incubation. Especially, there was a 49.70% (from 25.13 mg/kg to 12.64 mg/kg) reduction in acid soluble state and a 94.14% (from 12.98 mg/kg



◀**Fig. 3** The effects of SSB on the distribution of Cd form in soil. **a** Blank, **b** 1% SSB300, **c** 1% SSB500, **d** 3% SSB300, **e** 3% SSB500, **f** 5% SSB300, **g** 5% SSB500

kg to 25.20 mg/kg) increase in residual state for 5% SSB500 treatment in Fig. 3 (g). As observed in Fig. 3(f) and (g), 5% SSB500 was able to convert more of the Cd acid soluble state to the residual state than 5% SSB300. Additionally, in Fig. 3(c), (e), and (g), the passivation and stabilization of Cd became more effective with the application amount of SSB increased.

As shown in Fig. 4, SSB had the similar influence on Pb stabilization process compared with Cd. For all treatments with 60-day incubation, acid-soluble state in Cd and Pb both decreased significantly, whereas the relative residual state increased significantly. And the effect of 5% SSB500 was more obvious than the 1% and 3% application amount. Adding 5% SSB500 to the soil, the acid soluble state of Pb declined by 73.07% (from 27.37 mg/kg to 7.37 mg/kg), while the content of residual state increased by 93.21% (from 27.67 mg/kg to 53.46 mg/kg). Sun et al. (2021b) also found that Pb tended to be more stable with the formation of stable minerals at a higher SSB application amount (Sun, et al., 2021b).

As the results shown in Figs. 3 and 4, the higher application amount and pyrolysis temperature, the higher degree of passivation and stabilization of Cd and Pb in the soil. Wang et al. (2022) also found that As and Pb mobility in contaminated soil was reduced by the addition of sulfide FeO coated biochar in different pyrolysis temperatures and application amounts (Wang, et al., 2022). Tan et al. (2017) explored at different pyrolysis temperatures and the effect of pyrolysis temperature on the surface charge of SSB (Tan, et al., 2017). The negative charge on the surface of SSB gradually decreased with increasing temperature, while the fixation of Cd and Pb increased. Factors such as ash content, pH, oxygen-containing functional groups, polar groups, and hydrogen bonding of SSB could affect its surface charge. The determinants of surface charge were hydroxyl groups, and the hydroxyl group content declined with increasing temperature, leading to a reduction in negative surface charge (She et al., 2020). The pyrolysis temperature affected the chemical composition structure of SSB, causing changes in soil properties (specific surface area) and also differences in the adsorption

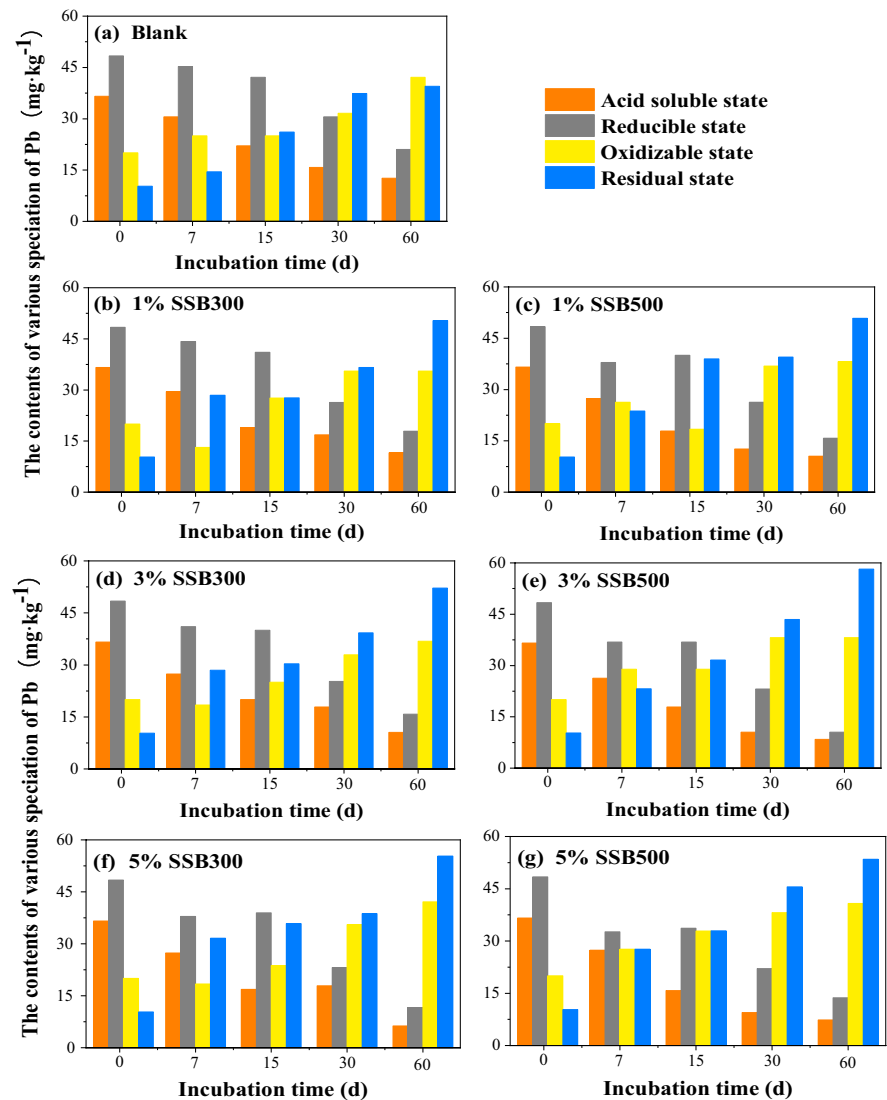
mechanism of heavy metals, thus remarkably influencing the availableness of SSB remediation of heavy metals.

### 3.4 Microbial Community Composition Analysis

Microorganisms were the leaders of various biogeochemical processes in soil (Xie, et al., 2021), and they were directly and indirectly affected by the content of soil heavy metals (Piotrowska-Seget, et al., 2004). Heavy metal contamination could reduce microbial abundance, diversity, and biochemical activity and alter community structure (Ellis et al., 2003). In the current study, the speciation of Cd and Pb in soil was responded by the abundance of microorganisms at the phylum and genus levels after 60-day incubation. As shown in Fig. S5, the Shannon index of soil samples incubated with 5% SSB500 increased significantly, reflecting the increase in microbial diversity in soil after 5% SSB500 application to soil (Ji, et al., 2020).

As seen in Fig. 5(a), the dominant phyla of bacteria in several groups of samples were *Proteobacteria*, *Actinobacteria*, *Firmicutes*, *Bacteroidetes*, and *Chloroflexi*. The presence of these microorganisms in large relative abundance demonstrated that they played an important role in heavy metal-contaminated soil and were well-adapted to extreme environments (Xie et al., 2021). The relative abundance of *Proteobacteria* in the 5% SSB500 added incubation group decreased from 31.9% to 24.9% compared to the blank group, when the bioavailable Cd and Pb contents were significantly lower, indicating a positive correlation between *Proteobacteria* and soil heavy metal content. The similar study by Gosai et al. (2018) found that *Proteobacteria* was more abundant in the samples contaminated with heavy metals (Gosai, et al., 2018) and this bacterium was highly tolerant to heavy metals (Guo, et al., 2019). From the perspective of *Proteobacteria*, it can be shown that 5% SSB500 had a good passivation and stabilization effect on soil Cd and Pb. As for the relative abundance of *Actinobacteria* (Zhu, et al., 2013), the increase of this bacterium was negatively correlated with the Cd content in the soil, and the relative abundance of *Actinobacteria* was significantly increased in the 5% SSB500 group, indicating a decrease in the toxicity of Cd in the soil after treatment with SSB500. The relative abundance of *Chloroflexi* in the soil applied with 5% SSB500 increased greatly. And

**Fig. 4** The effects of SSB on the distribution of Pb form in soil. **a** Blank, **b** 1% SSB300, **c** 1% SSB500, **d** 3% SSB300, **e** 3% SSB500, **f** 5% SSB300, **g** 5% SSB500



the results of DTPA and BCR evidenced that the bio-available state of Cd and Pb decreased significantly after 60-day incubation, as well as intensified the shift from the acid soluble state to the residual state of heavy metals. The results suggested that the relative abundance of *Chloroflexi* can reflect the reduction of heavy metal contamination in the soil. It was found that *Chloroflexi* could reduce heavy metal contamination, increase soil organic carbon content, and promote soil respiration through extracellular precipitation, cell wall adsorption, enzymatic oxidation, and intracellular complexation (Zhang, et al., 2020). Therefore, biologically effective heavy metals in soil could be reduced by cultivating *Chloroflexi* in soil,

providing an important supporting role for passivation and stabilizing soil heavy metal research through microbial perspective.

The relative abundance of microorganisms in different treatment groups at the genus level is shown in Fig. 5(b). The main genera with high relative abundance were *Bacillus*, *Defluviicoccus*, *Massilia*, *Lysobacter* (genus *Lysobacter*), *Sphingomonas*, *Pseudarthrobacter*, and *Flavisolibacter*. However, the other genera accounted for 35.6% and increased to 47.8% with the addition of 5% SSB500, indicating that the addition of SSB500 effectively increased the diversity of microorganisms in the soil. Because of its high specific surface area, SSB can be used as a carrier to



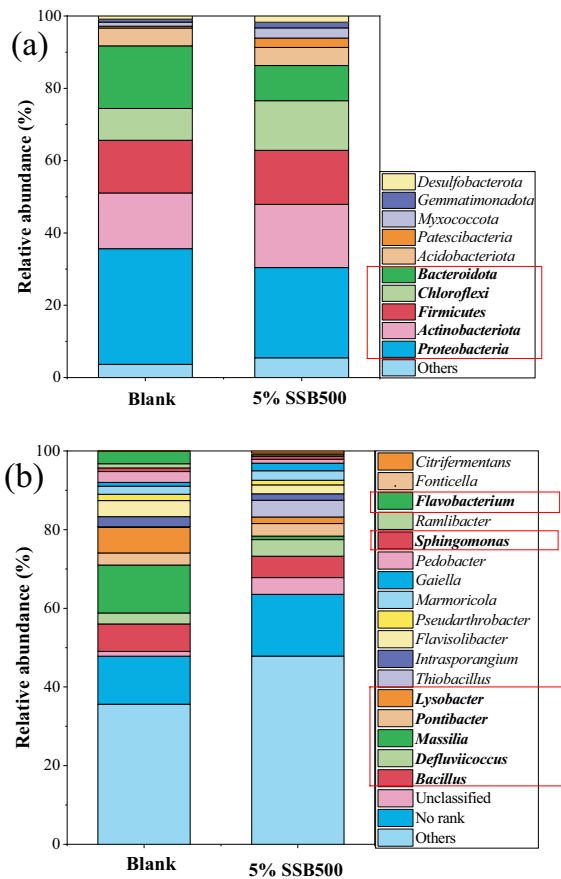


**Fig. 5** The effect of SSB on the relative abundance of soil microorganisms (**a** phylum level; **b** genus level)

enhance microbial adhesion and growth (Qin, et al., 2019). Among them, the relative abundance of *Massilia*, *Flavisolibacter*, and *Lysobacter* decreased by 11.3%, 4.9%, and 1.8%, respectively, after adding 5% SSB500. However, the relative abundance of *Thiobacillus* and *Defluviococcus* increased by 4.1% and 1.5%. This phenomenon was consistent with the findings of Li et al. (Liu, Zhang, et al., 2021). Han et al. (2020) have found that *Massilia* and *Lysobacter* were proportional to the concentration of Pb and Cd in the soil. *Thiobacillus* and *Defluviococcus* were genera commonly considered to be susceptible to heavy metals (Han, et al., 2020), inversely proportional to heavy metal concentrations (Hu, et al., 2021).

As reported, biochar not only can stabilize soil heavy metals, but also has a synergistic effect on the regulation and coupling of soil microorganisms. Similar results were obtained in this study. Overall,

the bioavailability of Cd and Pb in soil was significantly reduced when SSB500 was applied. The addition of 5% SSB500 had a better effect on the stability and soil properties of heavy metal, as 5% SSB500 can complex with heavy metals through a large number of organic functional groups, such as  $-\text{COOH}$  and  $-\text{OH}$  reaction, and reduce the concentration of soil Cd and Pb (Lan, et al., 2021). The reduction of heavy metal pollution can be observed from the perspective of microorganisms susceptible to heavy metals. In addition, the huge specific surface area and the complex microporous structure of 5% SSB500 provided binding sites for microorganisms (Li, et al., 2022), some of which were also involved in the stabilization of heavy metals. Generally, it was evident that the addition of SSB500 has reduced the bioavailability of Cd and Pb, which has led to the improvement of soil microbial community diversity (Liu, Zhang, et al., 2021).

When discussing changes in the composition of microbial communities, it was difficult to obtain differential information from simple community structure maps. Therefore, principal component analysis (PCA) was used to analyze microbial population information. As shown in Fig. 6, PCA analysis explained 88.70% of the variation in bacterial populations at the phylum level and 85.37% of the variation at the genus level. As shown in Fig. 6(a), after projecting the coordinate points of each sample, the relative abundance of SSB-treated samples at the genus level was greater in the direction of *Chloroflexi* and *Actinobacteria* than in Blank. *Actinobacteria* was identified to be able to participate in the iron cycle to produce Fe, which could be absorbed by other indigenous microorganisms to maintain their normal growth (Zhang, et al., 2019). In brief, the significant increase of the relative abundances of these functional bacterial communities could promote the soil nitrogen and carbon cycle, thus improving the reusability of the soil (Zhang, et al., 2021). As shown in Fig. 6(b), at the genus level, the Blank group in both the *Massilia* direction and the *Flavisolibacter* direction indicated that the relative abundance of these two genera was higher, while the soil with 5% SSB500 showed less relative abundance at both genus levels. The results reflected that the addition of 5% SSB500 significantly improved the microbial community structure, increased the relative abundance of beneficial microorganisms in the soil, and reduced the contamination

of soil with heavy metals to some extent. It was consistent with the conclusion of Han et al. (2017) that biochar could improve soil properties, inhibit soil acidification, and provide a carbon source to promote microbial growth (Han, et al., 2017). These results demonstrated that SSB500 was not only environmental-friendly, but was also beneficial to improve the diversity and composition of microbial community by increasing the bacterial abundances with heavy metal resistance.

#### 4 Conclusions

The preparation of sewage sludge into biochar and its application to heavy metal-contaminated soil solved the problem of outlet of sludge waste to a

certain extent, thus realizing the resource utilization of waste. The effect of SSB500 was better than that of SSB300, and the application of 5% SSB500 was better than that of 1% and 3%. As seen in the results of DTPA-extraction, the application of 5% SSB500 could reduce the bioavailability of Cd and Pb by 72.8% and 82.4%, respectively. The results of BCR-extraction showed that at higher pyrolysis temperature and application amount, more of the mobile state (acid soluble state) of Cd and Pb was converted to the stable fraction (residual state). In the soil incubation experiment, the acid soluble state of Cd was reduced by 49.70% (from 25.13 mg/kg to 12.64 mg/kg), while the residual state increased almost two-fold in the soil with 5% SSB500 (from 12.98 mg/kg to 25.19 mg/kg). Similarly, the acid soluble state of Pb decreased by 73.07% (from 27.37 mg/kg to 7.37 mg/kg), while the residual state increased by 93.21% (from 27.67 mg/kg to 53.46 mg/kg). Meanwhile, the addition of 5% SSB500 could act as a soil remediation and improve the diversity and species of soil microbial community within 60 days. At the phylum level, the relative abundance of *Chloroflexi* increased significantly, indicating that the bioavailability of Cd and Pb was reduced and the increase of easily available carbon sources would favor the growth of *Chloroflexi* in paddy soil. At the genus level, the significant increase in the relative abundance of *Defluviicoccus* reflected that the application of 5% SSB500 reduced the contamination of Cd and Pb in paddy soil. Microbial studies illustrate the synergistic stabilization of Cd and Pb by SSB and soil microorganisms, both of which microorganisms and SSB are indispensable.

**Acknowledgements** The authors would like to acknowledge the support provided by the State Key Laboratory of Pollution Control and Resource Reuse Foundation (No. PCRRF19001), and Natural Science Foundation of Shanghai (No. 22ZR1401700).

**Author Contribution** Huan Wang: conceptualization, formal analysis, methodology, data curation, and writing—original draft. Lei Zhou: writing—reviewing and editing. Yitong Dan: software. Xiaoxia Wang: validation and supervision. Yin-zhu Diao: investigation. Wenjing Sang: funding acquisition, resources, and writing—review and editing.

**Data Availability** The authors declare that all data supporting the findings of this study are available within the article and its supplementary information files.

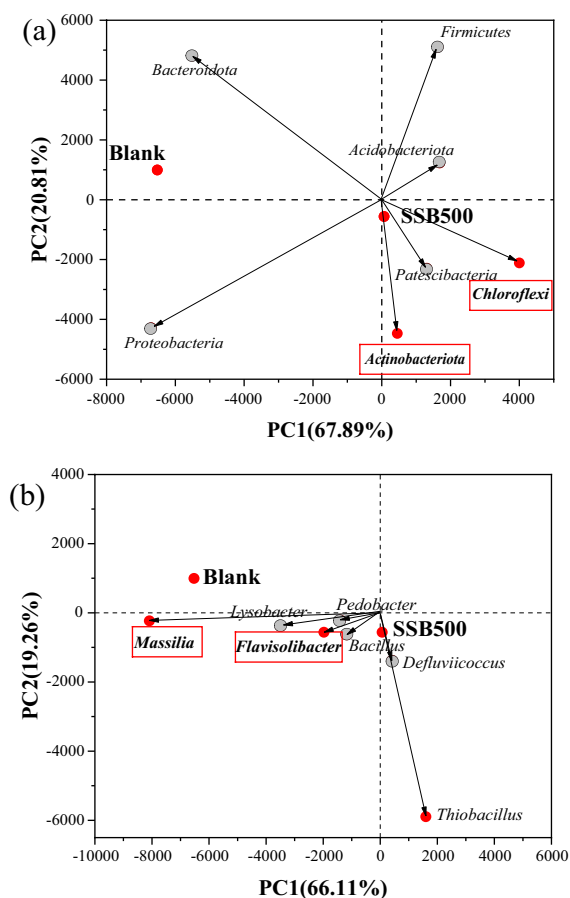


**Fig. 6** Principal component analysis (**a** phylum level; **b** genus level)

## Declarations

**Competing Interests** The authors declare no competing interests.

## References

- Beckers, F., Awad, Y. M., Beiyuan, J. Z., Abriagata, J., Mothes, S., Tsang, D. C. W., Ok, Y. S., & Rinklebe, J. (2019). Impact of biochar on mobilization, methylation, and ethylation of mercury under dynamic redox conditions in a contaminated floodplain soil. *Environment International*, *127*, 276–290. <https://doi.org/10.1016/j.envint.2019.03.040>
- Buha, A., Matovic, V., Antonijevic, B., Bulat, Z., Curcic, M., Renieri, E. A., Tsatsakis, A. M., Schweitzer, A., & Wallace, D. (2018). Overview of cadmium thyroid disrupting effects and mechanisms. *International Journal of Molecular Sciences*, *19*, 5. <https://doi.org/10.3390/ijms19051501>
- de Figueiredo, C. C., Chagas, J. K. M., da Silva, J., & Paz-Ferreiro, J. (2019). Short-term effects of a sewage sludge biochar amendment on total and available heavy metal content of a tropical soil. *Geoderma*, *344*, 31–39. <https://doi.org/10.1016/j.geoderma.2019.01.052>
- Eikelboom, M., Lopes, A. D. P., Silva, C. M., Rodrigues, F. D., Zanuncio, A. J. V., & Zanuncio, J. C. (2018). A multicriteria decision analysis of management alternatives for anaerobically digested kraft pulp mill sludge. *PLoS ONE*, *13*, 1. <https://doi.org/10.1371/journal.pone.0188732>
- Ellis, R. J., Philip, M., Weightman, A. J., & Fry, J. C. (2003). Cultivation-dependent and -independent approaches for determining bacterial diversity in heavy-metal-contaminated soil. *Applied and Environmental Microbiology*, *69*, 6. <https://doi.org/10.1128/AEM.69.6.3223-3230.2003>
- Fang, S. E., Tsang, D. C. W., Zhou, F. S., Zhang, W. H., & Qiu, R. L. (2016). Stabilization of cationic and anionic metal species in contaminated soil using sludge-derived biochar. *Chemosphere*, *149*, 263–271. <https://doi.org/10.1016/j.chemosphere.2016.01.060>
- Gao, R., Hu, H., Fu, Q., Li, Z., Xing, Z., Ali, U., Zhu, J., & Liu, Y. (2020). Remediation of Pb, Cd, and Cu contaminated soil by co-pyrolysis biochar derived from rape straw and orthophosphate: Speciation transformation, risk evaluation and mechanism inquiry. *Science of the Total Environment*, *730*, 139119. <https://doi.org/10.1016/j.scitotenv.2020.139119>
- Gosai, H. B., Sachaniya, B. K., Panseriya, H. Z., & Dave, B. P. (2018). Functional and phylogenetic diversity assessment of microbial communities at Gulf of Kachchh, India: An ecological footprint. *Ecological Indicators*, *93*, 65–75. <https://doi.org/10.1016/j.ecolind.2018.04.072>
- Guo, Q. W., Li, N. N., & Xie, S. G. (2019). Heavy metal spill influences bacterial communities in freshwater sediments. *Archives of Microbiology*, *201*(6), 847–854. <https://doi.org/10.1007/s00203-019-01650-y>
- Han, G. M., Lan, J. Y., Chen, Q. Q., Yu, C., & Bie, S. (2017). Response of soil microbial community to application of biochar in cotton soil with different continuous cropping years. *Sci Rep-Uk.*, *7*, 10184. <https://doi.org/10.1038/s41598-017-10427-6>
- Han, H., Wu, X. J., Yao, L. G., & Chen, Z. J. (2020). Heavy metal-immobilizing bacteria combined with calcium polypeptides reduced the uptake of Cd in wheat and shifted the rhizosphere bacterial communities. *Environmental Pollution*, *267*, 115432–115432. <https://doi.org/10.1016/j.envpol.2020.115432>
- D. Hopkins and K. Hawboldt, 2020. Biochar for the removal of metals from solution: A review of lignocellulosic and novel marine feedstocks. *Journal of Environmental Chemical Engineering* *8* (4). <https://doi.org/10.1016/j.jece.2020.103975>
- Hu, X. S., Liu, X. X., Qiao, L. K., Zhang, S., Su, K. W., Qiu, Z. L., Li, X. H., Zhao, Q. C., & Yu, C. H. (2021). Study on the spatial distribution of ureolytic microorganisms in farmland soil around tailings with different heavy metal pollution. *Science of the Total Environment*, *775*, 144946–144946. <https://doi.org/10.1016/J.SCITOTENV.2021.144946>
- Irfan, M., Ishaq, F., Muhammad, D., Khan, M. J., Mian, I. A., Dawar, K. M., Muhammad, A., Ahmad, M., Anwar, S., Ali, S., Khan, F. U., Khan, B., Bibi, H., Kamal, A., Musarat, M., Ullah, W., & Saeed, M. (2021). Effect of wheat straw derived biochar on the bioavailability of Pb, Cd and Cr using maize as test crop. *Journal of Saudi Chemical Society*, *25*, 5
- Islam, M. S., Kwak, J. H., Nzediegwu, C., Wang, S. Y., Palansuriya, K., Kwon, E. E., Naeth, M. A., El-Din, M. G., Ok, Y. S., & Chang, S. X. (2021). Biochar heavy metal removal in aqueous solution depends on feedstock type and pyrolysis purging gas. *Environmental Pollution*, *281*, 117094–117094. <https://doi.org/10.1016/J.ENVPOL.2021.117094>
- Ji, M., Sang, W., Tsang, D. C. W., Usman, M., Zhang, S., & Luo, G. (2020). Molecular and microbial insights towards understanding the effects of hydrochar on methane emission from paddy soil. *Science of the Total Environment*, *714*, 136769. <https://doi.org/10.1016/j.scitotenv.2020.136769>
- Jörg, R., Shaheen, S. M., Ali, E.-N., Hailong, W., Gijs, D. L., Alessi, D. S., & Yong, S. O. (2020). Redox-induced mobilization of Ag, Sb, Sn, and Tl in the dissolved, colloidal and solid phase of a biochar-treated and untreated mining soil. *Environment International*, *140*, 105754. <https://doi.org/10.1016/j.envint.2020.105754>
- Khanam, R., Kumar, A., Nayak, A. K., Shahid, M., Tripathi, R., Vijayakumar, S., Bhaduri, D., Kumar, U., Mohanty, S., Panneerselvam, P., Chatterjee, D., Satapathy, B. S., & Pathak, H. (2020). Metal(loid)s (As, Hg, Se, Pb and Cd) in paddy soil: Bioavailability and potential risk to human health. *Science of the Total Environment*, *699*, 134330. <https://doi.org/10.1016/j.scitotenv.2019.134330>
- Kong, S., Tang, J., Ouyang, F., & Chen, M. (2021). Research on the treatment of heavy metal pollution in urban soil based on biochar technology. *Environmental Technology & Innovation*, *23*. <https://doi.org/10.1016/J.ETI.2021.101670>
- Lam, S. S., Yek, P. N. Y., Ok, Y. S., Chong, C. C., Liew, R. K., Tsang, D. C. W., Park, Y. K., Liu, Z. L., Wong, C.

- S., & Peng, W. X. (2020). Engineering pyrolysis biochar via single-step microwave steam activation for hazardous landfill leachate treatment. *Journal of Hazardous Materials*, 390, 121649. <https://doi.org/10.1016/j.jhazmat.2019.121649>
- Lan, J. R., Zhang, S. S., Dong, Y. Q., Li, J. H., Li, S. Y., Feng, L., & Hou, H. B. (2021). Stabilization and Passivation of Multiple Heavy Metals in Soil Facilitating by Pinecone-Based Biochar: Mechanisms and Microbial Community Evolution. *Journal of Hazardous Materials*, 420, 126588. <https://doi.org/10.1016/j.jhazmat.2021.126588>
- Li, F., Wu, X., Ji, W., Gui, X., Chen, Y., Zhao, J., Zhou, C., & Ren, T. (2020). Effects of pyrolysis temperature on properties of swine manure biochar and its environmental risks of heavy metals. *Journal of Analytical and Applied Pyrolysis*, 152, 104945. <https://doi.org/10.1016/j.jaap.2020.104945>
- Li, J. H., Xia, C. G., Cheng, R., Lan, J. R., Chen, F. Y., Li, X. L., Li, S. Y., Chen, J. A., Zeng, T. Y., & Hou, H. B. (2022). Passivation of multiple heavy metals in lead-zinc tailings facilitated by straw biochar-loaded N-doped carbon aerogel nanoparticles: Mechanisms and microbial community evolution. *Science of the Total Environment*, 803, 149866. <https://doi.org/10.1016/j.scitotenv.2021.149866>
- Liu, W. L., Gong, Y. J., Chen, W. N., Liu, Z. Q., Wang, H., & Zhang, J. (2020a). Coordinated charging scheduling of electric vehicles: A mixed-variable differential evolution approach. *Ieee T Intell Transp.*, 21(12), 5094–5109. <https://doi.org/10.1109/TITS.2019.2948596>
- Liu, W., Xiao, Y., Zheng, T., & Chen, G. X. (2020b). Neural mechanisms of paroxysmal kinesigenic dyskinesia: Insights from neuroimaging. *Journal of Neuroimaging*. <https://doi.org/10.1111/JON.12811>
- Liu, L. H., Huang, L., Huang, R., Lin, H., & Wang, D. Q. (2021a). Immobilization of heavy metals in biochar derived from co-pyrolysis of sewage sludge and calcium sulfate. *Journal of Hazardous Materials*, 403, 123648–123648. <https://doi.org/10.1016/j.jhazmat.2020.123648>
- Liu, W. J., Graham, E. B., Dong, Y., Zhong, L. H., Zhang, J. W., Qiu, C. W., Chen, R. R., Lin, X. G., & Feng, Y. Z. (2021b). Balanced stochastic versus deterministic assembly processes benefit diverse yet uneven ecosystem functions in representative agroecosystems. *Environmental Microbiology*, 23(1), 391–404. <https://doi.org/10.1111/1462-2920.15326>
- Liu, Y. S., Zhang, Q. L., Cao, Y. Z., Yang, X., Li, Z. Y., Liu, W. H., Habyarimana, J. B., Cui, Y. K., Wang, H. Y., & Yang, R. T. (2021c). Effect of intermittent purge on O<sub>2</sub> production with rapid pressure swing adsorption technology. *Adsorption*, 27(2), 181–189. <https://doi.org/10.1007/s10450-020-00284-7>
- Mansoor, S., Kour, N., Manhas, S., Zahid, S., Wani, O. A., Sharma, V., Wijaya, L., Alyemeni, M. N., Alsahli, A. A., El-Serehy, H. A., Paray, B. A., & Ahmad, P. (2021). Biochar as a tool for effective management of drought and heavy metal toxicity. *Chemosphere*, 271, 129458. <https://doi.org/10.1016/J.CHEMOSPHERE.2020.129458>
- Meier, S., Curaqueo, G., Khan, N., Bolan, N., Cea, M., Eugenia, G. M., Cornejo, P., Ok, Y. S., & Borie, F. (2017). Chicken-manure-derived biochar reduced bioavailability of copper in a contaminated soil. *Journal of Soil and Sediments*, 17(3), 741–750. <https://doi.org/10.1007/s11368-015-1256-6>
- Mishra, S., Lin, Z., Pang, S., Zhang, Y., Bhatt, P., & Chen, S. (2021). Biosurfactant is a powerful tool for the bioremediation of heavy metals from contaminated soil. *Journal of Hazardous Materials*, 418, 26253–26253. <https://doi.org/10.1016/J.JHAZMAT.2021.126253>
- Otunola, B. O., & Ololade, O. O. (2020). A review on the application of clay minerals as heavy metal adsorbents for remediation purposes. *Environmental Technology & Innovation*, 18, 100692–100692. <https://doi.org/10.1016/j.eti.2020.100692>
- Piotrowska-Seget, Z., Cycoń, M., & Kozdroj, J. (2004). Metal-tolerant bacteria occurring in heavily polluted soil and mine spoil. *Applied Soil Ecology*, 28(3), 237–246. <https://doi.org/10.1016/j.apsoil.2004.08.001>
- Qin, X., Huang, Q. Q., Liu, Y. Y., Zhao, L. J., Xu, Y. M., & Liu, Y. T. (2019). Effects of sepiolite and biochar on microbial diversity in acid red soil from southern China. *Chemical Ecology*, 35(9), 846–860. <https://doi.org/10.1080/02757540.2019.1648441>
- Qu, M. J., Liu, G. L., Zhao, J. W., Li, H. D., Liu, W., Yan, Y. P., Feng, X. H., & Zhu, D. W. (2020). Fate of atrazine and its relationship with environmental factors in distinctly different lake sediments associated with hydrophytes. *Environmental Pollution*, 256, 113371. <https://doi.org/10.1016/j.envpol.2019.113371>
- Quan, W., Shaheen, S. M., Yahui, J., Ronghua, L., Michal, S., Hamada, A., Eilhann, K., Nanthi, B., Jörg, R., & Zeng-qiang, Z. (2021). Fe/Mn- and P-modified drinking water treatment residuals reduced Cu and Pb phytoavailability and uptake in a mining soil. *Journal of Hazardous Materials*, 403, 123628–123628. <https://doi.org/10.1016/j.jhazmat.2020.123628>
- She, X. D., Zhang, L. L., Peng, J. W., Zhang, J. Y., Li, H. B., Zhang, P. Y., Calderone, R., Liu, W. D., & Li, D. M. (2020). Mitochondrial complex I core protein regulates cAMP signaling via phosphodiesterase Pde2 and NAD homeostasis in *Candida albicans*. *Frontiers in Microbiology*, 11. <https://doi.org/10.3389/fmicb.2020.559975>
- Shentu, J. L., Li, X. X., Han, R. F., Chen, Q. Q., Shen, D. S., & Qi, S. Q. (2022). Effect of site hydrological conditions and soil aggregate sizes on the stabilization of heavy metals (Cu, Ni, Pb, Zn) by biochar. *Science of the Total Environment*, 802, 149949–149949. <https://doi.org/10.1016/J.SCIOTENV.2021.149949>
- Sun, T., Xu, Y. M., Sun, Y. B., Wang, L., Liang, X. F., & Jia, H. T. (2021a). Crayfish shell biochar for the mitigation of Pb contaminated water and soil: Characteristics, mechanisms, and applications. *Environmental Pollution*, 271. <https://doi.org/10.1016/J.ENVPOL.2020.116308>
- Sun, T., Xu, Y., Sun, Y., Wang, L., Liang, X., & Zheng, S. (2021b). Cd immobilization and soil quality under Fe-modified biochar in weakly alkaline soil. *Chemosphere*, 280, 130606. <https://doi.org/10.1016/J.CHEMOSPHERE.2021.130606>
- Tan, Z. X., Wang, Y. H., Zhang, L. M., & Huang, Q. Y. (2017). Study of the mechanism of remediation of

- Cd-contaminated soil by novel biochars. *Environ Sci Pollut r.*, 24(32), 24844–24855. <https://doi.org/10.1007/s11356-017-0109-9>
- Thakare, M., Sarma, H., Datar, S., Roy, A., Pawar, P., Gupta, K., Pandit, S., & Prasad, R. (2021). Understanding the holistic approach to plant-microbe remediation technologies for removing heavy metals and radionuclides from soil. *Current Research in Biotechnology.*, 3, 84–98. <https://doi.org/10.1016/j.crbiot.2021.02.004>
- Tian, S. Q., Wang, L., Liu, Y. L., & Ma, J. (2020). Degradation of organic pollutants by ferrate/biochar: Enhanced formation of strong intermediate oxidative iron species. *Water Research.*, 183, 116054. <https://doi.org/10.1016/j.watres.2020.116054>
- Tomczyk, B., Siatecka, A., Gao, Y. Z., Ok, Y. S., Bogusz, A., & Oleszczuk, P. (2020). The conversion of sewage sludge to biochar as a sustainable tool of PAHs exposure reduction during agricultural utilization of sewage sludges. *Journal of Hazardous Materials.*, 392, 122416. <https://doi.org/10.1016/j.jhazmat.2020.122416>
- Wang, Y. Y., Liu, Y. D., Zhan, W. H., Zheng, K. X., Wang, J. N., Zhang, C. S., & Chen, R. H. (2020). Stabilization of heavy metal-contaminated soil by biochar: Challenges and recommendations. *Science of the Total Environment.*, 729, 139060. <https://doi.org/10.1016/j.scitotenv.2020.139060>
- Wang, J., Sun, C., Huang, Q. X., Chi, Y., & Yan, J. H. (2021a). Adsorption and thermal degradation of microplastics from aqueous solutions by Mg/Zn modified magnetic biochars. *Journal of Hazardous Materials.*, 419, 126486. <https://doi.org/10.1016/j.jcoenv.2020.111261>
- Wang, J., Shi, L., Zhai, L., Zhang, H., Wang, S., Zou, J., Shen, Z., Lian, C., & Chen, Y. (2021b). Analysis of the long-term effectiveness of biochar immobilization remediation on heavy metal contaminated soil and the potential environmental factors weakening the remediation effect: A review. *Ecotoxicology and Environmental Safety.*, 207, 111261. <https://doi.org/10.1016/j.jcoenv.2020.111261>
- Wang, Z., Shen, R., Ji, S., Xie, L., & Zhang, H. (2021c). Effects of biochar derived from sewage sludge and sewage sludge/cotton stalks on the immobilization and phytoavailability of Pb, Cu, and Zn in sandy loam soil. *Journal of Hazardous Materials.*, 419, 126468. <https://doi.org/10.1016/J.JHAZMAT.2021.126468>
- Wang, G. H., Peng, C., Tariq, M., Lin, S., Wan, J., Liang, W. Y., Zhang, W., & Zhang, L. H. (2022). Mechanistic insight and bifunctional study of a sulfide FeO coated biochar composite for efficient As(III) and Pb(II) immobilization in soil<sub>34</sub>. *Environmental Pollution.*, 293, 118587. <https://doi.org/10.1016/j.envpol.2021.118587>
- Xie, Y., Bu, H., Feng, Q., Wassie, M., Ameer, M., Jiang, Y., Bi, Y., Hu, L., & Chen, L. (2021). Identification of Cd-resistant microorganisms from heavy metal-contaminated soil and its potential in promoting the growth and Cd accumulation of bermudagrass. *Environmental Research.*, 200, 111730. <https://doi.org/10.1016/J.ENVRES.2021.111730>
- Xing, J., Li, L. C., Li, G. B., & Xu, G. R. (2019). Feasibility of sludge-based biochar for soil remediation: Characteristics and safety performance of heavy metals influenced by pyrolysis temperatures. *Ecotox Environ Safe.*, 180, 457–465. <https://doi.org/10.1016/j.jcoenv.2019.05.034>
- Xu, D. Y., Gao, B., Gao, L., Zhou, H. D., Zhao, X. J., & Yin, S. H. (2016). Characteristics of cadmium remobilization in tributary sediments in Three Gorges Reservoir using chemical sequential extraction and DGT technology. *Environmental Pollution.*, 218, 1094–1101. <https://doi.org/10.1016/j.envpol.2016.08.062>
- Yang, Q. Q., Li, Z. Y., Lu, X. N., Duan, Q. N., Huang, L., & Bi, J. (2018). A review of soil heavy metal pollution from industrial and agricultural regions in China: Pollution and risk assessment. *Science of the Total Environment.*, 642, 690–700. <https://doi.org/10.1016/j.scitotenv.2018.06.068>
- Yang, C. D., Liu, J. J., & Lu, S. G. (2021). Pyrolysis temperature affects pore characteristics of rice straw and canola stalk biochars and biochar-amended soil. *Geoderma.*, 397, 115097
- Yang, Q. S., Masek, O., Zhao, L., Nan, H. Y., Yu, S. T., Yin, J. X., Li, Z. P., & Cao, X. D. (2021). Country-level potential of carbon sequestration and environmental benefits by utilizing crop residues for biochar implementation. *Applied Energy.*, 282, 116275. <https://doi.org/10.1016/j.apenergy.2020.116275>
- Yuan, H., Lu, T., Huang, H., Zhao, D., Kobayashi, N., & Chen, Y. (2015). Influence of pyrolysis temperature on physical and chemical properties of biochar made from sewage sludge. *Journal of Analytical and Applied Pyrolysis.*, 112, 284–289. <https://doi.org/10.1080/03650340.2017.1407870>
- Zhang, L. M., Zeng, Q., Liu, X., Chen, P., Guo, X. X., Ma, L. Y. Z., Dong, H. L., & Huang, Y. (2019). Iron reduction by diverse actinobacteria under oxic and pH-neutral conditions and the formation of secondary minerals. *Chemical Geology.*, 525, 390–399. <https://doi.org/10.1016/j.chemgeo.2019.07.038>
- Zhang, L., Zhang, P., Yoza, B. D., Liu, W., & Liang, H. (2020). Phytoremediation of metal-contaminated rare-earth mining sites using *Paspalum conjugatum*. *Chemosphere.*, 259, 127280. <https://doi.org/10.1016/j.chemosphere.2020.127280>
- Zhang, Y. Y., Yan, C. C., Liu, H. J., Pu, S. Y., Chen, H. L., Zhou, B. H., Yuan, R. F., & Wang, F. (2021). Bacterial response to soil property changes caused by wood ash from wildfire in forest soil around mining areas: Relevance of bacterial community composition, carbon and nitrogen cycling. *Journal of Hazardous Materials.*, 412, 125246. <https://doi.org/10.1016/j.jhazmat.2021.125246>
- Zhang, X., Zhao, B. W., Liu, H., Zhao, Y., & Li, L. J. (2022). Effects of pyrolysis temperature on biochar's characteristics and speciation and environmental risks of heavy metals in sewage sludge biochars. *Environmental Technology & Innovation.*, 26, 102288. <https://doi.org/10.1016/j.eti.2022.102288>
- Zhao, F. J., Ma, Y. B., Zhu, Y. G., Tang, Z., & McGrath, S. P. (2015). Soil contamination in China: Current status and mitigation strategies. *Environmental Science and Technology.*, 49(2), 750–759. <https://doi.org/10.1021/es5047099>
- Zhou, D., Liu, D., Gao, F. X., Li, M. K., & Luo, X. P. (2017). Effects of biochar-derived sewage sludge on heavy metal adsorption and immobilization in soil. *Int J Env Res Pub He.*, 14(7), 681. <https://doi.org/10.3390/ijerph14070681>
- Zhu, J., Zhang, J., Li, Q., Han, T., Xie, J., Hu, Y., & Chai, L. (2013). Phylogenetic analysis of bacterial community

composition in sediment contaminated with multiple heavy metals from the Xiangjiang River in China. *Marine Pollution Bulletin*, 70(1–2), 134–139. <https://doi.org/10.1016/j.marpolbul.2013.02.023>

Zhu, X. M., Chen, B. L., Zhu, L. Z., & Xing, B. S. (2017). Effects and mechanisms of biochar-microbe interactions in soil improvement and pollution remediation: A review. *Environmental Pollution*, 227, 98–115. <https://doi.org/10.1016/j.envpol.2017.04.032>

**Publisher's Note** Springer Nature remains neutral with regard to jurisdictional claims in published maps and institutional affiliations.